Influence of the structural incorporation of Er and Tb in different titania matrices on their photoluminescence properties.

André Estêvão, Luis F. Santos and Rui M. Almeida

Departamento de Engenharia Química, Insituto Superior Técnico, Universidade de Lisboa. Av.Rovisco Pais, nº1, 1049-001 Lisboa, Portugal

A B S T R A C T

Rare-earth doped titania bulk samples have been prepared by sol–gel processing. Erbium or Terbium oxides were incorporated in three different concentrations: 1 mol%, 3 mol% and 5 mol%. The samples were then subjected to different heat treatments to study the crystallization process. Thermal analysis results showed an increase in the crystallization temperature with increasing doping concentration. The diffractograms of the undoped titania samples indicate the presence of an amorphous phase at 300 ºC, the anatase phase at 350 ºC and the rutile phase at 500 ºC. Erbium or Terbium oxide doping yielded a remarkable stabilization of the anatase phase, since the rutile phase transformation temperature now occurs at 1050 ºC. For the higher doped samples, anatase and rutile crystallization is also accompanied by the formation of a pyrochlore phase, $Tb_2Ti_2O_7$/$Er_2Ti_2O_7$. FTIR spectroscopy revealed the presence of OH groups at ~3500 cm^{-1} and ~1600 cm^{-1}, in the amorphous phase, which led to a quenching effect and a strong reduction of the photoluminescence of the erbium-doped samples. The upconversion results of erbium doped crystalline titania samples showed an increase in the red emission when compared to the green emission, for higher doping concentrations, especially for the anatase matrix. For the terbium doped samples, the emission spectra yielded a much stronger emission in the amorphous matrix.

Keywords - Sol-gel; Photoluminescence; Titania matrix; Green / red emission; Quenching; Lanthanides.

1. Introduction

Titania, or titanium dioxide, is a well-known material used in several applications such as photocatalysis, photovoltaic, sunscreen or even as a white pigment used for painting or coloring. This oxide has three most known crystallographic polymorphs: Rutile, Anatase and Brookite [1] and, depending on certain factors as calcination temperature, presence of a dopant, synthesis method, and precursor used, anatase or rutile can be obtained in most scenarios [2]. The anatase to rutile transformation depends on several parameters such as the grain size, its shape, surface area, heating rate, impurities, volume of the sample and present atmosphere, among others [3]. It is widely reported that anatase to rutile transformation occurs in a range between 600 and 1000 ºC [4][5]. Among all synthesis methods, including hydrolysis of $TiCl_4$, flame pyrolysis, solvothermal or hydrothermal synthesis, chemical vapor deposition or physical vapor deposition [3], anodization, electrospinning, spin coating, atomic layer deposition, electrochemical deposition, direct oxidation and pulsed laser deposition [6], sol-gel processing is considered a low-cost technique and reproducible at large scale, with possibility for films deposition or multilayered structures [7], being also advantageous for studies of bulk or optical films with luminescent properties. The most important aspects considered for the matrix, when doped with lanthanide ions, are its high refractive index and high transparency which arise from low phonon energy. Using these two factors, the probability of non-radiative decay is lowered and increased the luminescence quantum yield [8], which can be defined as a ratio between emitted and absorbed photons.

2. Methods

2.1 Materials and synthesis

For the preparation of the titania sol, the precursor used was TPOT (titanium (IV)-propoxide, $Ti(OC_3H_7)_4$, Aldrich, 98%), together with glacial acetic acid (GAA) (Alfa Aesar, 99.+%) and Ethanol (Merck, 99.5%), used as solvents. The preparation of titania sol starts with 3 mL of GAA and, while stirring it

at low rotation, 2.5 mL of TPOT is added, dropwise, and stirred for 1h at room temperature (*RT*), called Sol.A. For undoped solutions, 18 mL of absolute ethanol was added and stirred for another 10 min, called Sol.C. For doped solutions, erbium nitrate penthydrate (*Sigma Aldrich;*99:9%*; Er*(NO_3)$_3$.5H_2O) or terbium chloride hexahydrate (*Sigma Aldrich;*99.9%*;TbCl*$_3$*:6*H_2O) were added to absolute ethanol, accomplishing the stoichiometric proportions, and dispersed by ultrasonication, Sol.D. The final solutions, C and D, were aged at RT to its gelation, taking approximately two weeks (figure 1) [9]. The samples prepared had the nominal composition (in mol%): (100-x)TiO_2–(x)$TbO_{1.5}$ and (100-x)TiO_2–(x)$ErO_{1.5}$,where x=1, 3 or 5. All compositions are expressed on a molar basis. Heat treatment (HT) was performed at 300 ºC, 350 ºC, 400 ºC, 500 ºC, 850 ºC and 1050 ºC on a HT time from 1-4 h.

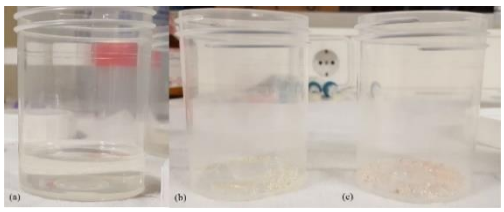

Figure 1: Titania Sol; Erbium and terbium doped titania gel.

2.2 Structural and microstructural characterization

Differential scanning calorimetry was performed on a DSC Q200 equipment, from Thermal Analytics, and nitrogen (*Air Liquide*) was used as flowing inert purge gas at the rate of 50 mL/min. For crystallographic phase identification the x-ray diffraction constituted by a Philips PW 3020 diffractometer, using CuKα radiation with a wavelength of 1.542 Å, a power of 30 W and a current of 40 mA. All measures were obtained with 2θ ranging between 10-70 º, an increment of 0.02 º and 1 s per step, in continuous mode. Surface view was analyzed through scanning electron micrographs taken with a FEG-SEM JEOL JSM-7001F equipment, in secondary electrons mode. For the Raman spectroscopy it was used a confocal micro-spectrophotometer Raman (Labram Evolution HR from Jobin Yvon Technology, Horiba), using a 532 nm diode laser (mpc6000, Laser Quantum) as excitation source, 10mW power in the sample, a grating of 600 lines/mm and a detection range of 100 to 1800 cm^{-1}. FT-IR Nicolet 5700 spectrophotometer from Thermo Electron Corporation was employed, using a KBr beamsplitter to the IR source, for the MIR region (4000 to 350 cm^{-1}) and a DTGS-TEC detector. An attenuated total reflection (*ATR*) accessory was used, using a single point ATR with a diamond crystal.

2.3. Luminescence characterization

Photoluminescence (*PL*) measurements in the infrared (900-1700 *nm*) were obtained using an Avantes spectrophotometer (AvaSpec-NIR256-1.7), excited by a 975 nm wavelength diode laser (*LumicsLU*0975*T* 080 - *D*605*N*12*A*), at 1W power, collected by an optical fiber (1401031 FC-UVIR600-2). Fluorolog-3, from HORIBA Jobin Yvon, was used to record photoluminescence spectra in the visible region, for terbium doped samples. The equipment was set with a range between 200-530 nm for an excitation spectrum and an excitation radiation of λ_{exc} = 484*nm* for the emission spectra. The radiation was obtained through a xenon lamp, in a continuous wave and a slit about 10 nm. UC photoluminescence spectra was recorded between 400 and 950 nm using a diode laser (*LumicsLU*0975*T* 080 - *D*605*N*12*A*) at 1W power, with excitation at 975 nm. The laser was focused on sample by a 10× micro-objective (*NA* = 28) and the generated UC PL was collected by a multimode fiber and guided into a spectrometer (0.85 m double monochromator, Spex 1403) and a photomultiplier tube detector (*Hamamatsu;R*928).

3. Results & discussion

3.1 DSC results

For the undoped titania sample, the DSC results indicated a crystallization onset temperature around 269 ºC and an increase of this temperature for doped titania samples as represented in table 1.

Table 1: Crystallization onset temperatures for undoped and erbium/terbium doped TiO_2 samples.

	Mol%	*Crystallization onset temperature (ºC)*
Undoped	0	269
Erbium doped	1	320
	3	346
	5	364
Terbium doped	1	337
	3	340
	5	376

For all terbium doped titania samples, it is observed an endothermic peak, around 100 ºC, assigned to the water release and an exothermic peak assigned to the crystallization reaction. For all erbium doped titania samples, in addition to those peaks found before, there are two exothermic peaks assigned to the removal of organics as represented in figure 2.

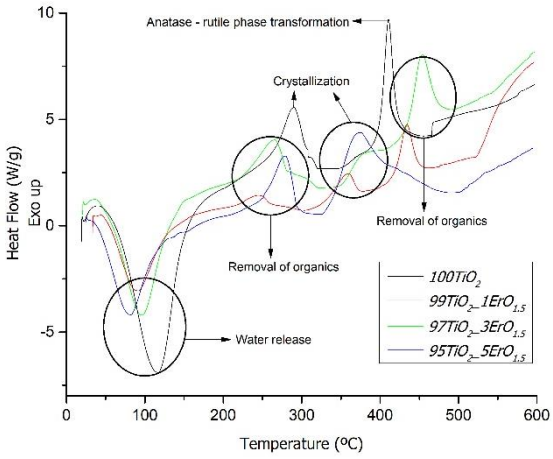

Figure 2: DSC curves of undoped and terbium doped titania bulk samples.

3.2 XRD results

Several HT temperatures were tested in order to determine the temperature at each phase was dominant. Considering XRD of the undoped sample, 100TiO_2, five different heat treatment temperatures, at 300 ºC, 350 ºC, 500 ºC, 850 ºC and 1050 ºC, were tested and samples were subjected to X-ray diffraction, which can be observed in figure 3. The diffractogram from 100TiO_2-HT300 sample showed a fully amorphous material. For a HT at 500ºC, 100TiO_2-HT500, both anatase and rutile phases were obtained, with the first to be the dominant over the mixture. This phase transformation is earlier than expected according to literature [3][10]. For a HT temperature of 850 ºC, 100TiO_2-HT850, a fully phase transformation to rutile occurs. For 1 mol% of erbium doped, there is mainly an anatase phase present for this HT temperature, which shows a delay for the phase transformation upon erbium incorporation. Furthermore, at higher temperatures, like 99TiO_2-1$ErO_{1.5}$-HT1050, rutile is the main phase present, together with a small content of a pyrochlore phase, $Er_2Ti_2O_7$, a faced center cubic crystal system. This pyrochlore phase is essentially affected by the dopant concentration and calcination temperature [11]. Upon increasing erbium concentration to

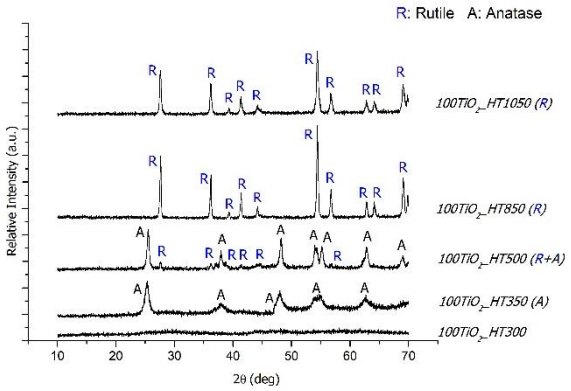

Figure 3: Undoped TiO_2 diffractograms, for different HT temperatures.

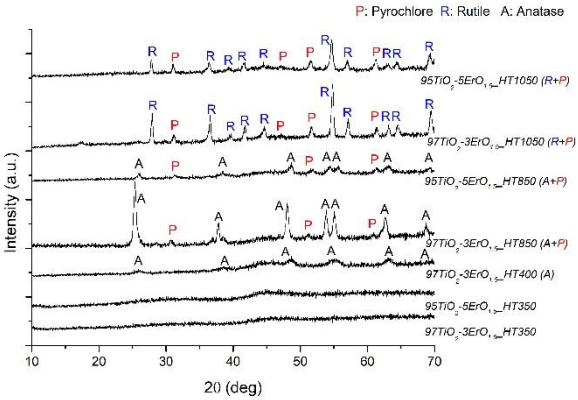

Figure 4: 97TiO_2-$ErO_{1.5}$ and 95TiO_2-5$ErO_{1.5}$ diffractograms, for different HT temperatures.

3 and 5%mol the crystallization of anatase phase is retarded and, for both compositions, it is possible to obtain an amorphous material at 350 ºC (figure 4) and such results corroborate the DSC findings.

The XRD results of terbium doped titania samples (not present in this report) present the same behavior as the erbium doped titania. As before, for 1 mol% of terbium doped titania, the characteristic HT temperatures for an amorphous, anatase and rutile phase are 300ºC, 850ºC and 1050ºC respectively, while for 3% and 5%mol are considered the HT temperatures at 350 ºC, 850 ºC and 1050 ºC.

The crystallite size was estimated using Scherrer's equation [23]:

$$D = \frac{K\lambda}{\beta\cos\theta}, \qquad \text{(eq.1)}$$

where D is the crystallite size in nanometers, K=0.89, λ is the x-ray wavelength, θ the diffraction angle and β is the corrected full width at half maximum, using an $\beta inst = 0.16$. The average size for terbium and erbium doped anatase samples is 21 nm which is a similar value as the anatase undoped titania sample, 20 nm. For doped and undoped rutile samples the same happens, where the average crystallite size is about 36 nm. In general,

there is a maintenance of crystallite sizes for doped and undoped samples. It became quite evident the growth of a pyrochlore phase for higher doping concentrations. In figure 4 it is noticed a decrease of relative intensities of rutile/pyrochlore upon increasing doping concentrations and HT temperature.

In the case of $99TiO_2$-$1ErO_{1.5}$-HT1050, the intensity of the pyrochlore phase peak is much lower than the rutile phase. However, for higher doping concentrations as $95TiO_2$-$5ErO_{1.5}$-HT1050, both phases present

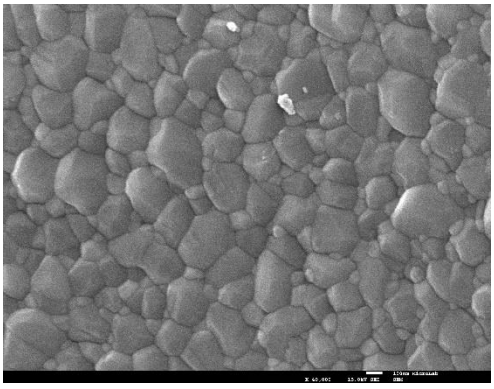

Figure 5: SEM surface image of $95TiO_2$-$5TbO_{1.5}$-HT1050 bulk samples (Scale bar of 100 nm).

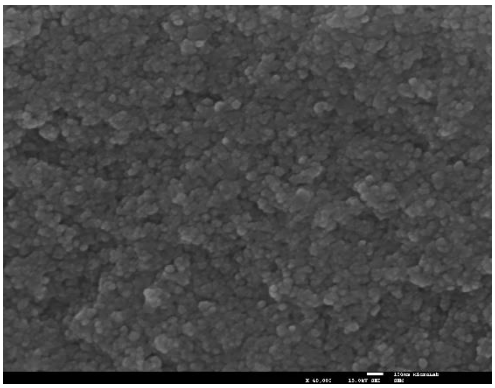

Figure 6: SEM surface image of $95TiO_2$-$5TbO_{1.5}$-HT850 bulk samples (Scale bar of 100 nm).

diffraction peaks with almost the same intensity counts, evidencing the growth of such pyrochlore phase.

3.3 SEM results

It is expected that an increase in the Er^{3+} content would inhibit the crystal growth of anatase phase, according to works of Iscoa et al. [10]. That was proven through SEM surface images observation, for terbium doped titania samples heat treated at 850 ºC. The grains have a lower size, about 20-50nm (figure 6), when compared to a rutile matrix phase, figure 5. In $99TiO_2$-$1TbO_{1.5}$-HT1050 sample, the particle size increased to 50-600nm and in $95TiO_2$-$5TbO_{1.5}$-HT1050 samples the particles sizes are ranging between 50-400 nm. This size decrease is attributed to the higher dopant concentration, which is an anatase phase stabilizer, retarding the anatase to rutile phase transformation and the particle's growth. Comparing the crystallite sizes with grain sizes, it is concluded that such calculations are just comparable when in a presence of an anatase matrix. The photoluminescence spectra are then expected to have a higher intensity in erbium and terbium doped samples when in a presence of an anatase matrix, rather than rutile, due to the smaller particle size [11].

3.3 FT-IR spectroscopy

In order to obtain an amorphous titania phase, for the $99TiO_2$-$1ErO_{1.5}$ sample, the maximum HT temperature was 300ºC since at 350ºC an anatase phase was already formed. Even with a 2/4 hours HT time, the results get quite similar to a single hour of HT. A large band centered at ~3350 cm^{-1} gets quite evident in figure 7, together with the ~1630 cm^{-1} peak, attributed to the OH bending vibrations of molecular water [12]. When doped with 3 mol% of erbium these bands disappear, however at 5 mol% those bands are present again, an indication of the difficulty to obtain free OH samples. All samples present a drop-in transmittance bellow 1000 cm^{-1}, corresponding to the Ti–O–Ti vibration. According to Salhi et al. [13] this band is centered at 450 cm^{-1}. Also, a peak at ~ 2920 and ~ 2850 cm^{-1} is also present, mainly in $97TiO_2$-$3ErO_{1.5}$ sample, assigned to the CH_3 and CH_2 asymmetric and symmetric

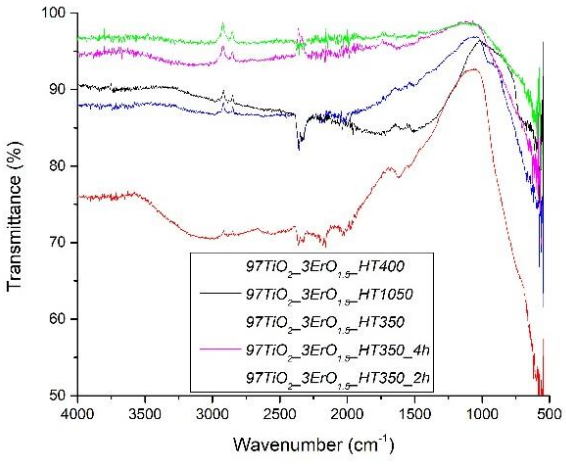

Figure 7: $97TiO_2$-$3ErO_{1.5}$ bulk samples: FTIR-ATR spectra.

vibrations, respectively [18]. These bands are not related to the samples since it also was observed in a sample heat treated at 1050 ºC and should be then related to any sort of equipment contamination as ethanol or acetone. This sample is used as a reference for a free-OH content material.

3.4 Photoluminescence results

In the $99TiO_2$-$1ErO_{1.5}$ sample spectra, it is notorious the absence of any peak on the sample $99TiO_2$-$1ErO_{1.5}$-*HT*300, in figure 8. The lack of luminescent properties is attributed to OH^- content by means non-radiative emissions. There is an absorption from the ground state to the energy level ${}^4I_{11/2}$, represented by the transition ${}^4I_{15/2} \rightarrow {}^4I_{11/2}$, but the quenching effect promoted by this group led to the ${}^4I_{11/2} \rightarrow {}^4I_{13/2}$ transition, followed by a non-radiative emission, ${}^4I_{13/2} \rightarrow {}^4I_{15/2}$, by the hydroxyl groups through an energy transfer. When increasing HT temperature up to 500 ºC, the peaks correspondent to 526, 532, 547 and 553 nm emissions are present in the green region, while the red region is characterized by 661, 670 and 678 nm emissions. For such emissions there is an excitation from the ground state to an excited state by means of GSA, ${}^4I_{15/2} \rightarrow {}^4I_{11/2}$, followed by excited state absorption (ESA) or energy transfer up-conversion (ETU) mechanism, by the ${}^4I_{11/2} \rightarrow {}^4F_{7/2}$ transition. Through relaxation processes, there are non-radiative emissions and decay to lower levels such as the emission related to the peak at 525nm by ${}^2H_{11/2} \rightarrow {}^4I_{15/2}$, at 540 and 565nm by the ${}^4H_{3/2} \rightarrow {}^4I_{15/2}$ transition. The emissions in the red region are characterized by the further relaxation from higher energy levels or by a first relaxation

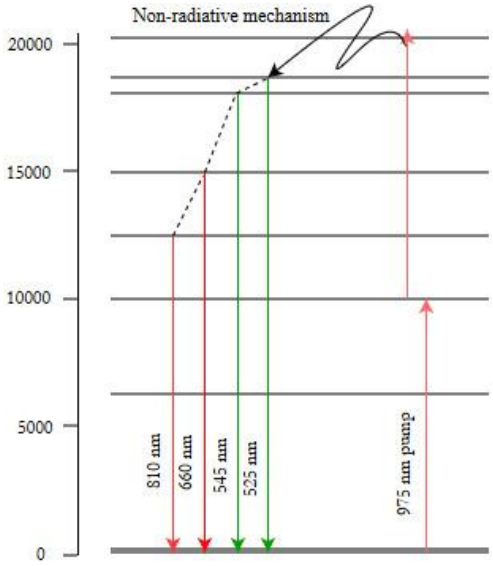

Figure 9: Erbium electronic transitions upon excitation at 975 nm. Adapted from [16].

from ${}^4I_{11/2} \rightarrow {}^4I_{13/2}$ and ESA, ${}^4I_{13/2} \rightarrow {}^4F_{9/2}$ [16]. Two emissions were detected, at 660 and 675nm, correspondent to the ${}^4F_{9/2} \rightarrow {}^4I_{15/2}$ transition [17][14]. The sample $99TiO_2$-$1ErO_{1.5}$-*HT*1050 has four sharp emission peaks in the green region, at 524, 547, 555 and 566nm, while in the red region it is at 651, 656, 658, 661, 673 and 678 nm [19], with respect to the same transitions written before. These emissions are well known and studied in literature from recent years, especially for erbium doped samples [14] [15],

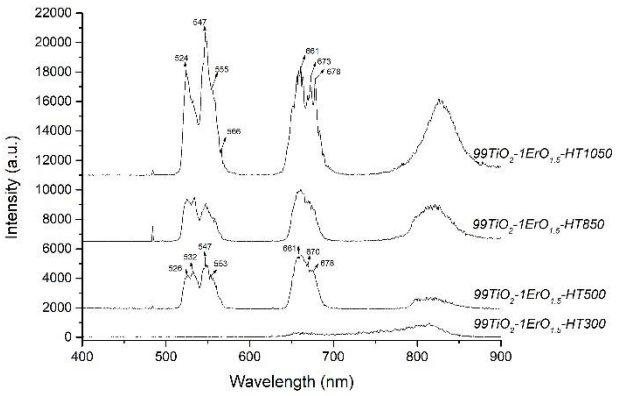

Figure 8: Up-conversion spectra of $99TiO_2$-$1ErO_{1.5}$, for different HT temperatures. Excitation at 975 nm.

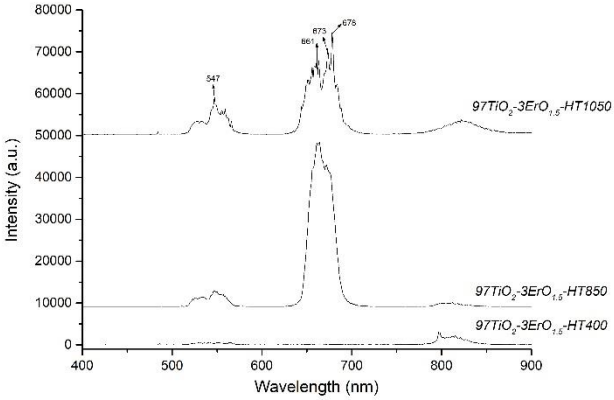

Figure 10: Up-conversion spectra of $97TiO_2$-$3ErO_{1.5}$, for different HT temperatures. Excitation at 975 nm.

represented in figure 9. The stark splitting here is more evident than at any other HT temperature. For all $99TiO_2$-$1ErO_{1.5}$ bulk samples it is obtained a spectrum where red and green intensities, and respectively integrated areas, are quite similar, in samples where there is a rutile or anatase phase. For such doping concentration, it remains the

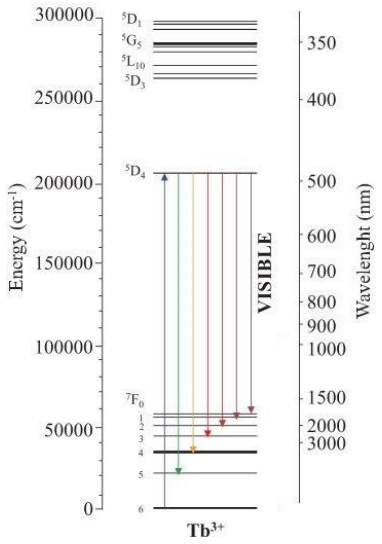

Figure 11: Terbium electronic transitions upon excitation at 484 nm.

487nm, $^5D_4 \rightarrow {}^4F_5$ at 543nm, $^5D_4 \rightarrow {}^4F_4$ at 583nm, $^5D_4 \rightarrow {}^4F_3$ at 621nm, $^5D_4 \rightarrow {}^4F_2$ at 646nm, $^5D_4 \rightarrow {}^4F_1$ at 669nm and $^5D_4 \rightarrow {}^4F_0$ at 679nm, present in figure 12. The sample 99TiO_2-1Tb$O_{1.5}$-HT300 sample presents a broad band with a high intensity while both 99TiO_2-1Tb$O_{1.5}$-HT850 and 99TiO_2-1Tb$O_{1.5}$-HT1050 present three main peaks at 545, 586 and 622nm assigned to the $^5D_4 \rightarrow {}^4F_5$, $^5D_4 \rightarrow {}^4F_4$ and $^5D_4 \rightarrow {}^4F_3$ transitions, respectively, however with low intensities. This broad band from the sample 99TiO_2-1Tb$O_{1.5}$-HT300 is also expected since the excitation spectra presents a broad band with high intensities. Regarding 95TiO_2-5Tb$O_{1.5}$, which has an identical spectrum of 97TiO_2-3Tb$O_{1.5}$, it is possible to observe that, in presence of an amorphous phase, there are emissions at 646, 669 and 679 nm, as shown in figure 12. All these peaks are assigned to

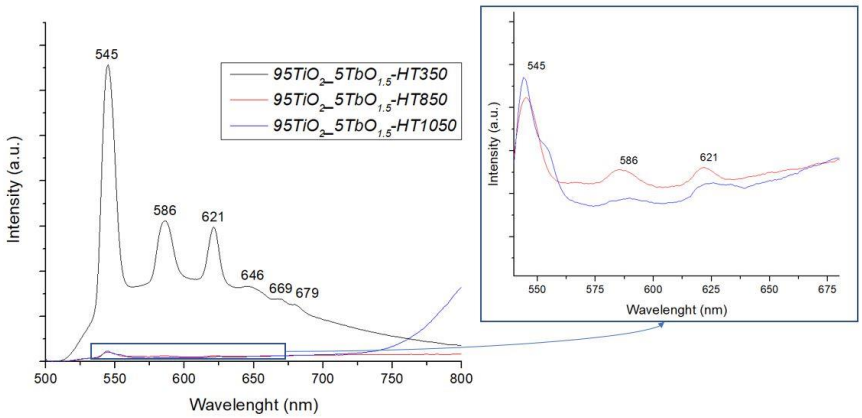

Figure 12: Emission spectra of 95TiO2-5TbO1.5 sample, for different HT temperatures. Excitation at 484 nm.

result of low intensity emissions. Considering 97TiO_2-3$ErO_{1.5}$, in figure 10, there is one major difference when compared to 99TiO_2-1$ErO_{1.5}$ emission spectra. The emission peaks associated with the transitions in the red region are much higher than for lower doping concentrations. All the emissions in the green region remain practically the same, in intensity and position, however the transitions at 661, 663 and 672nm are 11 times more intense with HT at 850 ºC and 5 times higher at 1050 ºC. This increase at red emission happens when a pyrochlore structure is formed. In 99TiO_2-1$ErO_{1.5}$ samples, which do not present this structure, there is a homogeneous emission intensity, denoting a quenching effect by the presence of this pyrochlore structure in higher doping concentrations.

Terbium photoluminescence was also studied by means of down-shifting. Upon an excitation at 484nm it is expected several emissions such as the $^5D_4 \rightarrow {}^4F_6$ transition at

$^5D_4 \rightarrow {}^4F_J$ transitions, when $J_{0\rightarrow5}$, as represented in figure 11. The peaks are narrow, the transitions are well defined and intense and, when compared to higher HT temperatures such as HT850 and HT1050, the intensity of the 545 nm emission is almost 28 times higher in an amorphous structure than crystallized forming structures as rutile and anatase. These results are supported by other studies where it was obtained higher intensities when in an amorphous phase [20]. A possible explanation for such behavior is that when the lanthanides are embedded in an amorphous matrix, the short-range structure makes it possible to obtain an unperturbed electronic structure and presenting sharp and narrow peaks. [21]. Moreover, the absence of a pyrochlore structure at this calcination temperature results in an exclusion of a concentration quenching effect, contrarily to 95TiO_2-5Tb$O_{1.5}$-HT850 and 95TiO_2-5Tb$O_{1.5}$-HT1050 samples. [22]

4. Conclusions

Titania and rare earth doped titania bulks, with 1; 3 and 5 mol% of erbium or terbium oxide, have been prepared by the sol–gel method. Heat treatment of undoped titania, indicated the presence of anatase and/or rutile, while for the doped compositions a pyrochlore phase was also observed. From the diffractograms obtained, it is possible to conclude that with increasing doping concentration, the crystallization temperatures increased and the amount of the pyrochlore phase also increased. Also, the phase transformation, from anatase to rutile, is retarded: in undoped titania samples the phase transformation temperature was ~ 500 ºC, while for erbium/terbium doped titania samples it was ~ 1050 ºC.

A crystallite size of 20-50 nm, estimated by the Scherrer equation, revealed similar values to the observed grain size obtained in SEM, for doped and undoped titania, apart from the terbium doped rutile, heat treated at 1050 ºC, where an increase in grain size to 50 - 600 nm was observed in SEM.

FTIR spectroscopy showed the presence of residual OH content, for samples where the presence of amorphous phase is observed, even after heat treatment. As a result, there was a strong quenching effect in the erbium-doped samples and they did not present photoluminescence properties.

The up-conversion results for erbium doped crystalline titania samples showed an intensification of the red emission, when compared to the green emission, for higher doping concentrations, especially in the anatase matrix. With increasing heat treatment temperature, Stark splittings are clearly observed, indicating a more strongly crystallized environment for erbium in the rutile phase, due to the formation of the pyrochlore phase.

On the other hand, the emission spectra of the terbium doped compositions yielded a much stronger intensity in the amorphous phase matrix, compared to the crystalline titania matrices.

5. References

[1] M. Memesa, S. Lenz, S. G. Emmerling, S. Nett, J. Perlich, P. Müller-Buschbaum, and J. S. Gutmann. "Morphology and photoluminescence study of titania nanoparticles." In: *Colloid and Polymer Science* 289.8 (2011), pp. 943–953. issn: 0303402X. doi: 10.1007/s00396-011-2421-0.

[2] D. Reyes-Coronado, G. Rodriguez Gattorno, M. E. Espinosa-Pesqueira, C. Cab, R. De Coss, and G. Oskam. "Phase-pure TiO_2 nanoparticles: Anatase, brookite and rutile." In: *Nanotechnology* 19.14 (2008). issn: 09574484. doi: 10.1088/0957-4484/19/14/145605

[3] D. A. Hanaor and C. C. Sorrell. "Review of the anatase to rutile phase transformation." In: *Journal of Materials Science* 46.4 (2011), pp. 855–874. issn: 00222461. doi: 10.1007/s10853-010-5113-0.

[4] R. Pandiyan, R. Bartali, V. Micheli, G. Gottardi, I. Luciu, D. Ristic, G. Alombert Goget, M. Ferrari, and N. Laidani. "Influence of Nd^{3+}doping on the structural and near-IR photoluminescence properties of nanostructured TiO_2 films." In: *Energy Procedia* 10 (2011), pp. 167–171. issn: 18766102. doi: 10.1016/j.egypro.2011. 10.171.

[5] L. Liang, Y. Yulin, Z. Mi, F. Ruiqing, Q. Lele,W. Xin, Z. Lingyun, Z. Xuesong, and H. Jianglong. "Enhanced performance of dye sensitized solar cells based on TiO_2 with NIR-absorption and visible up-conversion luminescence." In: *Journal of Solid State Chemistry* 198 (2013), pp. 459–465. issn: 00224596. doi: 10.1016/j.jssc.2012.10.013.

[6] B. Roose, S. Pathak, and U. Steiner. "Doping of TiO_2 for sensitized solar cells." In: *Chem. Soc. Rev.* 44.22 (2015), pp. 8326 -8349. issn: 0306-0012. doi: 10.1039/C5CS00352K

[7] R. E. Rojas-Hernandez, L. F. Santos, and R. M. Almeida. "$Tb^{3+/}Yb^{3+}$doped aluminosilicate phosphors for near infrared emission and efficient down-conversion." In: *Journal of Luminescence* 197.January (2018), pp. 180–186. issn: 00222313. doi: 10.1016/j.jlumin.2018.01.020.

[8] J. Chen and J. X. Zhao. "Upconversion nanomaterials: Synthesis, mechanism, and applications in sensing." In: *Sensors* 12.3 (2012), pp. 2414–2435. issn: 14248220. doi: 10.3390/s120302414.

[9] R. E. Rojas-Hernandez, N. P. Barradas, E. Alves, L. F. Santos, and R. M. Almeida. "Up-conversion emission of aluminosilicate and titania films doped with $Er^{3+/}Yb^{3+}$by ion implantation and sol-gel solution doping." In: *Surface and Coatings Technology* January (2018), pp. 0–1. issn: 02578972. doi: 10.1016/j.surfcoat.2018.01.056.

[10] P. Lopez-Iscoa, D. Pugliese, N. Boetti, D. Janner, G. Baldi, L. Petit, and D. Milanese. "Design, Synthesis, and Structure-Property Relationships of Er^{3+}-Doped TiO_2 Luminescent Particles Synthesized by Sol-Gel." In: *Nanomaterials* 8.1 (2018), p. 20. issn: 2079-4991. doi: 10.3390/nano8010020.

[11] J. Zhang, X. Wang, W. T. Zheng, X. G. Kong, Y. J. Sun, and X. Wang. "Structure

and luminescence properties of TiO2:Er3+ nanocrystals annealed at different temperatures." In: *Materials Letters* 61.8-9 (2007), pp. 1658–1661. issn: 0167577X. doi: 10.1016/j.matlet.2006.07.093.

[12] I. L. Vera Estrada, R Narro-García, T López-luke, V. H. Romero, J. A. Christen, and E De La Rosa. "Synthesis and luminescence properties of TiO_2: Yb–Er mesoporous nanoparticles." In: *Bulletin of Materials Science* 41.4 (2018), p. 110. issn: 0250-4707. doi: 10.1007/s12034-018-1615-1.

[13] R. Salhi and J. L. Deschanvres. "Efficient green and red up-conversion emissions in Er/Yb co-doped TiO2nanopowders prepared by hydrothermal-assisted sol–gel process." In: *Journal of Luminescence* 176 (2016), pp. 250 259. issn: 00222313. doi: 10.1016/j.jlumin.2016.03.011.

[14] I. Camps, M. Borlaf, J. Toudert, A. de Andrés, M. T. Colomer, R. Moreno, and R. Serna. "Evidencing early pyrochlore formation in rare-earth doped TiO_2 nanocrystals: Structure sensing via VIS and NIR Er3+light emission." In: *Journal of Alloys and Compounds* 735 (2018), pp. 2267–2274. issn: 09258388. doi: 10.1016/j.jallcom.2017.11.262.

[15] W. Luo, C. Fu, R. Li, Y. Liu, H. Zhu, and X. Chen. "Er^{3+}-doped anatase TiO_2 nanocrystals: Crystal-field levels, excited-state dynamics, upconversion, and defect luminescence."In: *Small* 7.21 (2011), pp. 3046–3056. issn: 16136810. doi: 10.1002/ smll.201100838.

[16] P. Jenouvrier, G. Boccardi, J. Fick, A. M. Jurdyc, and M. Langlet. "Up-conversion emission in rare earth-doped Y2Ti2O7sol-gel thin films." In: *Journal of Luminescence* 113.3-4 (2005), pp. 291–300. issn: 00222313. doi: 10.1016/j.jlumin.2004.10.025.

[17] Q. Shang, H. Yu, X. Kong, H. Wang, X. Wang, Y. Sun, Y. Zhang, and Q. Zeng. "Green and red up-conversion emissions of Er3+ Yb3+Co-doped TiO2nanocrystals prepared by sol-gel method." In: *Journal of Luminescence* 128.7 (2008), pp. 1211–1216. issn: 00222313. doi: 10.1016/j.jlumin.2007.11.097.

[18] P.Praven, G. Viruthagiri, S. Mugundan, and N. Shanmugam. "Structural, optical and morphological analyses of pristine titanium di-oxide nanoparticles – Synthesized via sol-gel route." In: *Spectrochimica Acta – Part A: Molecular and Biomolecular Spectroscopy* 117 (2014), pp. 622-629 issn: 13861425 doi: 10.1016/j.tsf.2013.09.037.

[19] W. Luo, C. Fu, R. Li, Y. Liu, H. Zhu, and X. Chen. "Er3+-doped anatase TiO2nanocrystals: Crystal-field levels, excited state dynamics, upconversion, and defect luminescence." In: *Small* 7.21 (2011), pp. 3046–3056. issn: 16136810. doi: 10.1002/ smll.201100838.

[20] A. A. Ismail, M. Abboudi, P. Holloway, and H. El-Shall. "Photoluminescence from terbium doped silica-titania prepared by a sol gel method." In: *Materials Research Bulletin* 42.1 (2007), pp. 137–142. issn: 00255408. doi: 10.1016/j.materresbull.2006.05.002.

[21] J. C. G. Bünzli and V. K. Pecharsky. "Preface." In: *Handbook on the Physics and Chemistry of Rare Earths* 53 (2018), pp. ix–xv. issn: 01681273. doi: 10.1016/S0168-1273(18)30013-8.

[22] I. Cacciotti, A. Bianco, G. Pezzotti, and G. Gusmano. "Terbium and ytterbiumdoped titania luminescent nanofibers by means of electrospinning technique." In: *Materials Chemistry and Physics* 126.3 (2011), pp. 532 541. issn: 02540584. doi: 10.1016/j.matchemphys.2011.01.034.

[23] J.Ferreira, L. F. Santos, and R.M. Almeida. *Active material development for Yb lase with applications in materials processing.* Tech. rep., pp-1-10